THE JOURNAL OF BIOLOGICAL CHEMISTRY VOL. 285, NO. 18, pp. 13863–13873, April 30, 2010

The Pax6b Homeodomain Is Dispensable for Pancreatic Endocrine Cell Differentiation in Zebrafish*[S]

Received for publication, January 27, 2010 Published, JBC Papers in Press, February 22, 2010, DOI 10.1074/jbc.M110.108019

Vincianne Verbruggen[‡1], Olivier Ek[‡], Daphné Georlette[§], François Delporte[‡], Virginie Von Berg[‡], Nathalie Detry[‡], Frédéric Biemar[§], Pedro Coutinho[¶], Joseph A. Martial[‡], Marianne L. Voz[‡2], Isabelle Manfroid[‡3], and Bernard Peers[‡2,3,4]

From the [‡]Unit of Molecular Biology and Genetic Engineering, University of Liège, GIGA-R, B34, Avenue de l'Hôpital 1, B-4000 Liège, Belgium, the [§]Department of Biology, Temple University, Philadelphia, Pennsylvania 19122, and the [¶]Medical Research Council Human Genetics Unit, Western General Hospital, Edinburgh EH4 2XV, Scotland, United Kingdom

Pax6 is a well conserved transcription factor that contains two DNA-binding domains, a paired domain and a homeodomain, and plays a key role in the development of eye, brain, and pancreas in vertebrates. The recent identification of the zebrafish *sunrise* mutant, harboring a mutation in the *pax6b* homeobox and presenting eye abnormalities but no obvious pancreatic defects, raised a question about the role of *pax6b* in zebrafish pancreas. We show here that *pax6b* does play an essential role in pancreatic endocrine cell differentiation, as revealed by the phenotype of a novel zebrafish *pax6b* null mutant and of embryos injected with *pax6b* morpholinos. Pax6b-depleted embryos have almost no β cells, a strongly reduced number of δ cells, and a significant increase of ε cells. Through the use of various morpholinos targeting intron-exon junctions, *pax6b* RNA splicing was perturbed at several sites, leading either to retention of intronic sequences or to deletion of exonic sequences in the *pax6b* transcript. By this strategy, we show that deletion of the Pax6b homeodomain in zebrafish embryos does not disturb pancreas development, whereas lens formation is strongly affected. These data thus provide the explanation for the lack of pancreatic defects in the *sunrise pax6b* mutants. In addition, partial reduction of Pax6b function in zebrafish embryos performed by injection of small amounts of *pax6b* morpholinos caused a clear rise in α cell number and in glucagon expression, emphasizing the importance of the fine tuning of the Pax6b level to its biological activity.

The transcription factor Pax6 is well conserved among metazoa and plays important roles in the development of several organs, including the eye, brain, pituitary, and pancreas (1–5). The protein contains two DNA-binding domains, a paired domain (PD)[5] and a paired-like homeodomain (HD), and the C-terminal proline-, serine-, and threonine-rich (PST) region, which is acting as a transcriptional activation domain. Many studies on the function of the murine *Pax6* gene rely on the analysis of $Pax6^{Sey}$ (small eye) and $Pax6^{Sey\text{-}Neu}$ mutant mice, harboring distinct point mutations in the *Pax6* coding region. These often lead to C-terminal truncations in the Pax6 protein, disrupting its activity (6–8). These truncated *Pax6* mutant mice exhibit a phenotype essentially identical to that of *Pax6/LacZ* knock-out mice (9) and are thus considered as null mutants. Although heterozygous *Pax6* mutants display eye malformations (reduced lens size, iris and corneal anomalies) and some forebrain patterning defects (10, 11), no obvious morphological abnormalities have been detected in the pancreas. Yet mice and human patients heterozygous for a *Pax6* mutation often display impaired glucose tolerance at the adult stage (12, 13). Rodents homozygous for a *Pax6* null mutation lack eye and olfactory bulbs, have severe brain anomalies, and display severe defects in the differentiation of pancreatic endocrine cells (7, 9, 14–18). Also, overexpression of *Pax6* within the eye, brain, or pancreas in transgenic mouse embryos perturbs the development of these organs, showing that an optimal level of PAX6 protein activity is crucial for proper organogenesis (19–21). In the murine pancreas, *Pax6* is expressed in all endocrine cell types, and its inactivation leads to significant depletion of insulin- and somatostatin-expressing cells (β cells and δ cells, respectively), almost total loss of glucagon-expressing cells (α cells), and a strong increase in ghrelin-expressing cells (ε cells) (9, 15, 22, 23).

Previous studies have shown that the PD is crucial for Pax6 function because a mutation causing a deletion within this domain leads to a phenotype of the eyes and brain almost identical to that of *Pax6* null mutants. On the other hand, the missense mutation $Pax6^{Neu4}$, leading to an amino acid substitution within the HD, preventing DNA binding through this domain, also affects eye development but causes only subtle defects in telencephalon development (18). These data suggest that most Pax6 target genes in the brain are regulated through the PD, whereas in the eye, the HD is also important. *In vivo* studies on the respective roles of the PD and HD in pancreatic cell differentiation have not yet been reported.

* This work was funded by the Belgian State Program on "Interuniversity Poles of Attraction" and by the 6th European Union Framework Program (Beta Cell Therapy Integrated Project).
[S] The on-line version of this article (available at http://www.jbc.org) contains supplemental Figs. S1–S4.
[1] Recipient of a doctoral fellowship from the "Fonds pour la Formation à la Recherche dans l'Industrie et l'Agriculture."
[2] "Chercheur Qualifié" from the "Fonds National pour la Recherche Scientifique."
[3] Both authors contributed equally to this work.
[4] To whom correspondence should be addressed. Tel.: 32-4-366-33-74; E-mail: bpeers@ulg.ac.be.

[5] The abbreviations used are: PD, paired domain; HD, homeodomain; PST, proline-, serine-, and threonine-rich; hpf, hours postfertilization; BSA, bovine serum albumin; RT, reverse transcription; dpf, days postfertilization.

Because of a genome duplication early in the evolution of teleost fish, two *pax6* genes exist in zebrafish. Both are active in ocular and brain structures, but only one, *pax6b*, is expressed in pancreatic endocrine cells because of sequence divergence within the pancreatic cis-regulatory regions (24, 25). Recently, the *sunrise* zebrafish mutant was reported to contain a deleterious missense mutation in the homeobox of the *pax6b* gene (24). Although homozygous *sunrise* mutant embryos display a microphthalmia (small eye) phenotype with abnormal lens and corneal structures, they display a normal number of α and β pancreatic cells, and adult *sunrise* mutants are viable and fertile (24). This surprising finding was in sharp contrast with the severe pancreatic defects observed in the Pax6 mutant mice and prompted us to investigate further the role of *pax6b* in zebrafish pancreas development. In the present study, we demonstrate the crucial role of Pax6b for the differentiation of endocrine cells in the zebrafish pancreas and, by using morpholinos disrupting *pax6b* mRNA splicing, we show that the Pax6b homeodomain is dispensable for pancreas development.

EXPERIMENTAL PROCEDURES

Transgenic Lines and Fish Maintenance—The AB strain, *pax6b*:GFP/insulin:*dsRed* (25) and the *ptf1a*:GFP (26, 27) transgenic lines, used for *pax6b* morpholino injections, were raised according to Ref. 35. All of the embryos were staged according to Kimmel *et al.* (28). The genotyping of *pax6b*^{sa0086} and *sunrise* embryos was done on DNA extracted from tails of ISH-stained embryos by performing nested PCR using primers as reported previously (24) and as recommended by the Zebrafish Mutation Resource (available on the Sanger Web site), respectively.

Whole Mount in Situ Hybridization—Single whole mount *in situ* hybridizations were performed as previously described by Hauptmann and Gerster (29). Antisense RNA probes were synthesized by transcription of cDNA clones with T7, T3, or SP6 RNA polymerase and using digoxigenin labeling mix (Roche Applied Science). The following probes were used: glucagon (30), insulin (31), somatostatin 2 (32), and ghrelin (NCBI number AL918922; digestion with ApaI and transcription with T3).[6]

Morpholino Injections—The antisense morpholino oligonucleotides of splicing (Gene Tools) used were as follows: Mo1Pax6b (5′-GGCTTCACAAGTCACCTGCAAAATC), Mo2Pax6b (5′-TTGATTTGCACTCACGCTCGGTATG), Mo3Pax6b (5′-AAAGTTGTGATCGTTCACCTTTCTC), Mo4Pax6b (5′-GGCAACCGTCTGCAAAAATATAACA), Mo5Pax6b (5′-TCGACACCTGAATGGACAGCAATAT), and Mo1mutArx (5′-GCGTCTTTATTAGCTCGTCAACACA) as control morpholino. These morpholinos target the exon-intron or intron-exon boundary. They were diluted in Danieau solution, from which 1000 pl were injected into the yolk of one-cell stage embryos. To check the injection efficiency, rhodamine dextran was added at 0.5% in the injected solution.

Control of the Morpholino Efficiency—Zebrafish embryos were injected at the one-cell stage with Mo1Pax6b (6 ng/embryo), Mo2Pax6b (4.5 ng/embryo), Mo3Pax6b (6 ng/embryo), Mo5Pax6b (2 ng/embryo), Mo2Pax6b plus Mo5Pax6b (4.5 ng + 2 ng/embryo), Mo3Pax6b plus Mo4Pax6b (6 ng + 4 ng/embryo), or an *arx*-mutated morpholino (1.7 ng/embryo). We performed a reverse transcription on 1 μg of mRNA extracted from these morpholino-injected embryos or from non-injected control embryos at 24 or 30 h postfertilization (hpf). The primers used for the PCR amplification on the obtained cDNA were as follows: *pax6b* paired domain (upstream primer, 5′-GAACGGCAGACCGTTACCGGACTC; downstream primer, 5′-CTCTGCCCGTTGAGCATTCTCAGC), *pax6b* homeodomain (upstream primer, 5′-GCAACAGATGGGTGCAGATGGC; downstream primer, 5′-CTGTATTCTTGCTTCCGGGAGGTC), and *nkx6.2* (upstream primer, 5′-TATTCTGGCCGGGAATGATG; downstream primer, 5′-GCCTCTTTCGCCATTTAGTTCTT). cDNAs were subjected to 30 or 40 cycles of 30 s at 94 °C, 30 s at 60 °C, and 30 s at 68 °C, followed by a final 7-min extension at 68 °C.

Pax6 Antibody, Immunofluorescence, and Western Blotting—Pax6 antibody was purified from rabbit antiserum after several injections of purified Pax6b C- terminal domain expressed in *Escherichia coli* (last 88 amino acids of Pax6b). This antibody reacts against both zebrafish Pax6a and Pax6b proteins. Immunofluorescence was performed on 22–24-hpf zebrafish embryos fixed in 2% paraformaldehyde using anti-Pax6 antibody (1:200) and Alexa-488 anti-rabbit (1:500; Molecular Probes, Inc. (Eugene, OR)) as secondary antibody. Briefly, washes were performed in PBS plus 0.3% Triton X-100, and antibody incubations were in PBS plus 0.3% Triton X-100 plus 4% BSA. For Western blotting, crude extracts were prepared from 40 zebrafish embryos injected with various morpholinos. One-fifth of extracts were loaded on an acrylamide gel, analyzed with the anti-Pax6 (1:200) or an anti-tubulin (1:1000; Abcam) as primary antibodies and then with the second horseradish peroxidase-coupled antibody (1:2000; Cell Signaling) and revealed with the ECL chemiluminescence kit (Pierce).

Imaging—Microscope pictures were performed with an Olympus DP70 photocamera fixed on a BX60 Olympus microscope. Pax6 immunostaining was captured with a Leica TCS SP2 laser confocal microscope. All of the pictures were processed using Adobe Photoshop and Adobe Illustrator software.

RNA Extraction, Reverse Transcription, and Quantitative PCR—Total RNA was extracted with Qiazol (Qiagen) from two different batches of 25 larvae injected with Mo2 or control morpholinos. cDNA was synthesized from 1 μg of total RNA by reverse transcription with the RT Transcriptor First Strand cDNA synthesis kit (Roche Applied Science) according to the manufacturer's instructions. One-twentieth of the resulting cDNA was used for real-time PCR with the one-step 2× Mastermix (Diagenode, Liège, Belgium) containing SYBR Green. Thermal cycling was performed on an Applied Biosystems 7000 detection system (Applied Biosystems, Foster City, CA). For all reactions, negative controls were run with no template present, and random RNA preparations were also subjected to sham quantitative RT-PCR (no reverse transcription) to verify lack of genomic DNA amplification. The relative transcript levels for the genes of interest (glucagon, insulin, and somatostatin transcripts) were obtained by the relative standard curve method and normalized with respect to the mean of two reference genes, *EF1α* and *Rpl13a*. Primers, the sequences of which are

[6] V. Verbruggen, unpublished results.

available upon request, were designed with Primer Express version 2.0 software (Applied Biosystems, Foster City, CA) and selected so as to span exon-exon junctions, to avoid detection of genomic DNA.

RESULTS

Pax6b Plays a Key Role in the Differentiation of Pancreatic Endocrine Cells in Zebrafish Embryos—To determine the function of Pax6b in the zebrafish pancreas, we first injected fertilized zebrafish eggs with an antisense morpholino (Mo2) annealing to the exon 6-intron 6 junction of the *pax6b* gene. This morpholino disrupts RNA splicing at that junction, causing the removal of exon 6 coding sequences in *pax6b* transcripts, leading to a frameshift and a premature stop codon in the paired domain (see Fig. 4 and see below for further detailed descriptions). Almost no full-length Pax6b protein could be detected in the pancreas of injected embryos by immunostaining, whereas expression of the paralog Pax6a protein was still easily detected in the neural tube by the same anti-C-terminal Pax6 antibody (Fig. 1, *A* and *B*). Formation of the different pancreatic endocrine cells was then analyzed in the Mo2 morphants at 3 days postfertilization (dpf) and compared with those of uninjected embryos or of embryos injected with an unrelated sequence morpholino used as a control. Almost no insulin-expressing β cells were detected in the Mo2 morphants, as opposed to an average of 25–35 insulin-expressing cells in control embryos (*Co*) (Fig. 1, *C* and *D*). The number of somatostatin-expressing cells was also drastically decreased in about 90% of the morphants (Fig. 1, *E* and *F*). Conversely, ghrelin-expressing cells were barely detectable in wild-type embryos but numerous and easily observed in all of the Mo2 morphants (Fig. 1, *G* and *H*). The number of glucagon-expressing cells was not significantly affected in the morphants injected with 4.5 ng of Mo2 (Fig. 1, *I* and *J*). However, injection of 9 ng of Mo2 morpholino resulted in a reproducible decrease of glucagon cells (data not shown). To determine whether *pax6b* knockdown affected development of the pancreatic exocrine tissue, Mo2 morpholino was injected in the *ptf1a:GFP* transgenic zebrafish line. No obvious change of the exocrine tissue could be detected in the morphants (Fig. 1, *K* and *L*), consistent with the lack of *pax6b* expression in these cells. Very similar endocrine pancreatic defects were observed when embryos were analyzed 30 hpf (supplemental Fig. S1).

The lost of β cells in the Mo2 morphants sharply contrasts with the apparent normal number of β cells reported in the zebrafish *pax6b sunrise* mutant at 5 dpf (24). Thus, we decided to further analyze the pancreatic phenotype of the *sunrise* mutants at 30 and 3 dpf. No difference could be detected between *sunrise* homozygous embryos and their wild-type siblings in the number of either α, β, δ, or ϵ cell types (supplemental Fig. S2). To confirm that the endocrine pancreatic defects in Mo2 morphants are due to the knockdown of *pax6b* and not of Mo2 off-targets, we analyzed the pancreas of a novel zebrafish *pax6b* mutant recently identified at the Zebrafish Mutant Resource (available on the World Wide Web). This *pax6b* mutant allele (*sa0086*) harbors a C to A substitution changing codon 109 (Tyr) to a premature stop codon. Thus, this allele encodes a Pax6b protein possessing a truncated

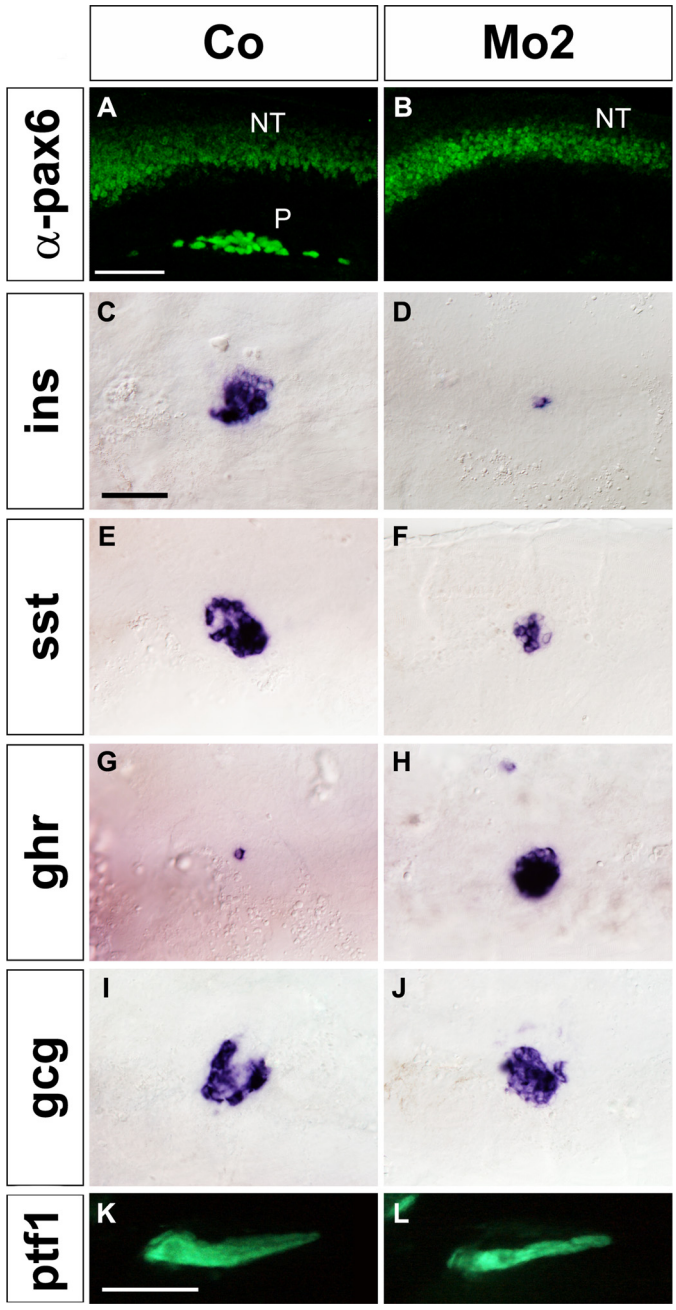

FIGURE 1. **Pancreatic function of the zebrafish *pax6b* gene.** *A* and *B*, Pax6 immunostaining of whole mount 1-dpf zebrafish embryos injected with a control morpholino (*A*) or with the *pax6b* Mo2 morpholino (4.5 ng/embryo) (*B*); Pax6b protein is not detected in pancreatic cells (*P*), whereas *pax6a* expression is not affected in the neural tube (*NT*) in the morphants. *C–L*, analysis of pancreatic markers in control embryos (*left column*) and in *pax6b* morphants (*right column*) by *in situ* hybridization. Ventral views of the pancreatic area of 3-dpf embryos are shown with the anterior side to the *left*. *ins*, insulin; *gcg*, glucagon; *sst*, somatostatin; *ghr*, ghrelin, *ptf1a* gene. The number of insulin- and somatostatin-expressing cells decreases in the *pax6b* morphants, whereas ghrelin expression increases. *Scale bar*, 50 μm (*A–J*) and 200 μm (*K* and *L*). *Co*, control embryos.

paired domain and lacking the whole homeodomain plus the transactivation C-terminal domain (Fig. 2). Based on the *pax6* allelic mutant series described in mammals and in *Drosophila*, the $pax6b_{sa0086}$ allele corresponds to a null mutation. Crosses between $pax6b_{sa0086}$ carrier fish generated homozygous mutant embryos, all displaying severe lens defects (Fig. 2, *A* and

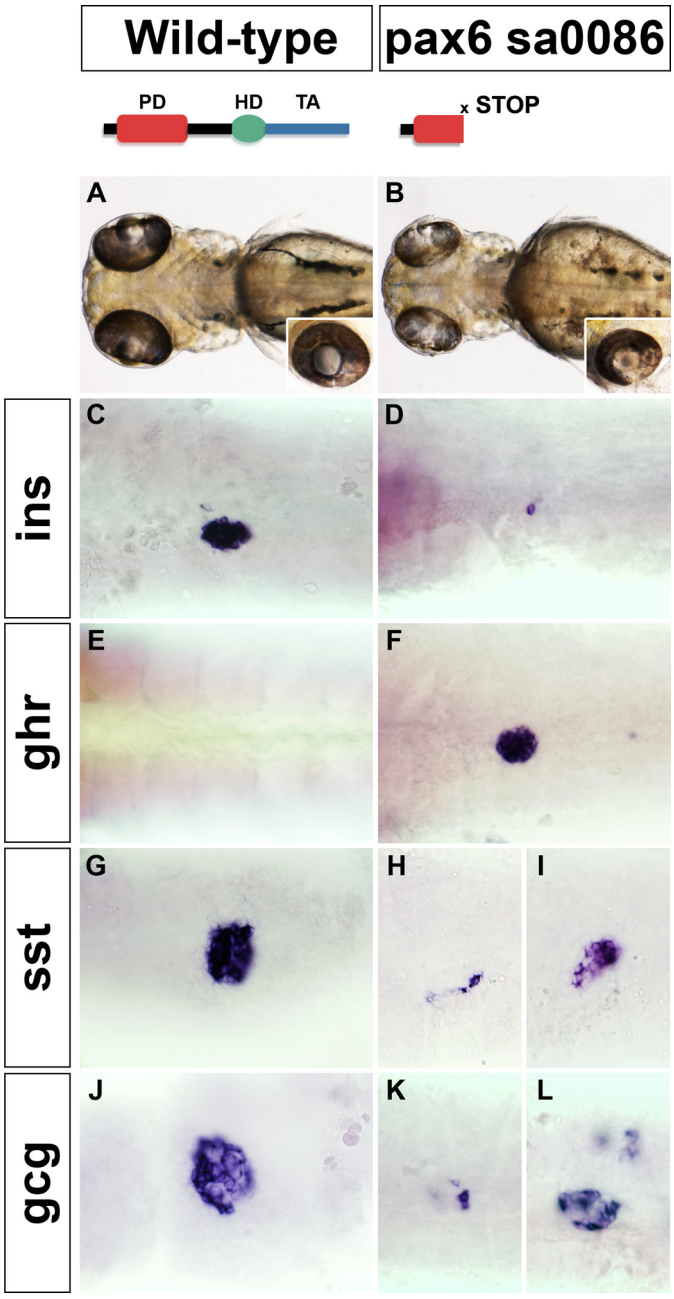

FIGURE 2. **Pancreatic cell endocrine differentiation is perturbed in *sa0086 pax6b*$^{-/-}$ zebrafish mutants.** *Top panels*, schematic drawing of Pax6 structures in wild type and *sa0086* mutant. *A–L*, phenotype comparison of wild-type (*left column*) and *sa0086* mutant (*right column*) 3- and 5-dpf larvae. *A* and *B*, eye and lens morphology; *C–L*, expression of pancreatic hormones by *in situ* hybridization. Ventral views of the pancreatic area are shown with the anterior side to the *left*. *ins*, insulin; *gcg*, glucagon; *sst*, somatostatin; *ghr*, ghrelin. The number of insulin and somatostatin cells are significantly reduced in the mutants, whereas ghrelin cells increase dramatically. A high variability is observed for glucagon expression among mutants.

B). However, the expressivity was variable, from a reduction of the lens size in some mutants to a complete lack of lens in others. The pancreatic phenotype of the homozygous *pax6b*^{sa0086} mutants was similar to the Mo2 morphants with almost an absence of β cells and a strong increase of ϵ cells in all homozygous mutants (Fig. 2, *C–F*). A marked diminution of somatostatin-expressing cells was also detected in mutants, as in Mo2 morphants, but the level of reduction varied between mutant embryos ($n = 14$), one mutant displaying a complete lack of δ cells, nine mutants containing 1–5 δ cells, and three possessing 6–10 δ cells (Fig. 2, *G–I*). With regard to glucagon-expressing α cells, some mutants were presenting with an almost normal level or a slight decrease of α cells ($n = 7$), whereas other mutants displayed a severe reduction ($n = 5$) (Fig. 2, *J–L*). Thus, the analysis of the *pax6b*^{sa0086} mutant strengthens the knockdown data, confirming the essential role of Pax6b in the differentiation of endocrine cells in the zebrafish pancreas.

Requirement of Similar Pax6b Levels for Lens and Pancreatic β Cell Development—Given the important role of Pax6b in the endocrine pancreas, the apparent normal pancreas of the *sunrise* mutant is quite surprising. One explanation might be that the *sunrise* missense mutation occurring in the *pax6b* homeobox is a hypomorphic mutation causing only partial loss of Pax6b activity, sufficient to produce morphological abnormalities in the eye but not sufficient to affect cell differentiation in the endocrine pancreas. To test this hypothesis, we injected zebrafish eggs with different amounts of *pax6b* Mo2 morpholino, and we examined the eyes and counted the number of insulin-expressing cells in each morphant (Fig. 3). We used a doubly transgenic zebrafish line harboring the insulin:*dsRed* transgene for monitoring the number of β cells and the *Pax6b*:*GFP* transgene for monitoring the entire endocrine pancreatic cell lineage and the retinal neurons. Expression of the endogenous insulin gene was also checked by whole mount *in situ* hybridization (inlets in the *bottom panels* of Fig. 3*A*). As the amount of injected Mo2 morpholino increased, the lens appeared increasingly smaller, almost disappearing at 4.5 ng (Fig. 3, *top panels*). Precise measurement of the lens surface for each experimental condition revealed a dose-dependent decrease (Fig. 2*B*). In parallel, a similar progressive reduction was also detected in the expression of both the insulin:*dsRed* transgene and the endogenous insulin gene. In contrast, the total number of pancreatic endocrine cells expressing the *Pax6b*:*GFP* transgene was not affected (Fig. 3, *middle panels*) (data not shown). Quantitative analyses showed that the morpholino dose required to reduce the lens size was the same as the dose required to reduce the number of β cells. Thus, the phenotypic difference between the *pax6b*^{sa0086} mutants and the *sunrise* mutants cannot be explained by different thresholds of Pax6 activity required for development of the eyes and of the pancreas.

Control of β, δ, and ϵ Cell Differentiation Does Not Require the Pax6b Homeodomain—Another hypothesis that might explain the phenotypic difference between *sunrise* mutants and the *pax6b*^{sa0086} mutants is that the DNA binding activity of Pax6b in pancreatic cells relies on the paired domain rather than on its homeodomain. This would explain why *sunrise* mutants, harboring a missense mutation within the Pax6b homeobox, display normal pancreatic cell differentiation. To test this hypothesis, we designed two other morpholinos, Mo3 and Mo4, targeting the intron-exon splicing junctions at both ends of exon 8 (Fig. 4, *top panels*). Exon 8 encodes the N-terminal region of the Pax6b homeodomain, containing the leucine 244 residue that is mutated in the *sunrise* mutant. Because this exon is 159 bp long, its deletion from *pax6b*

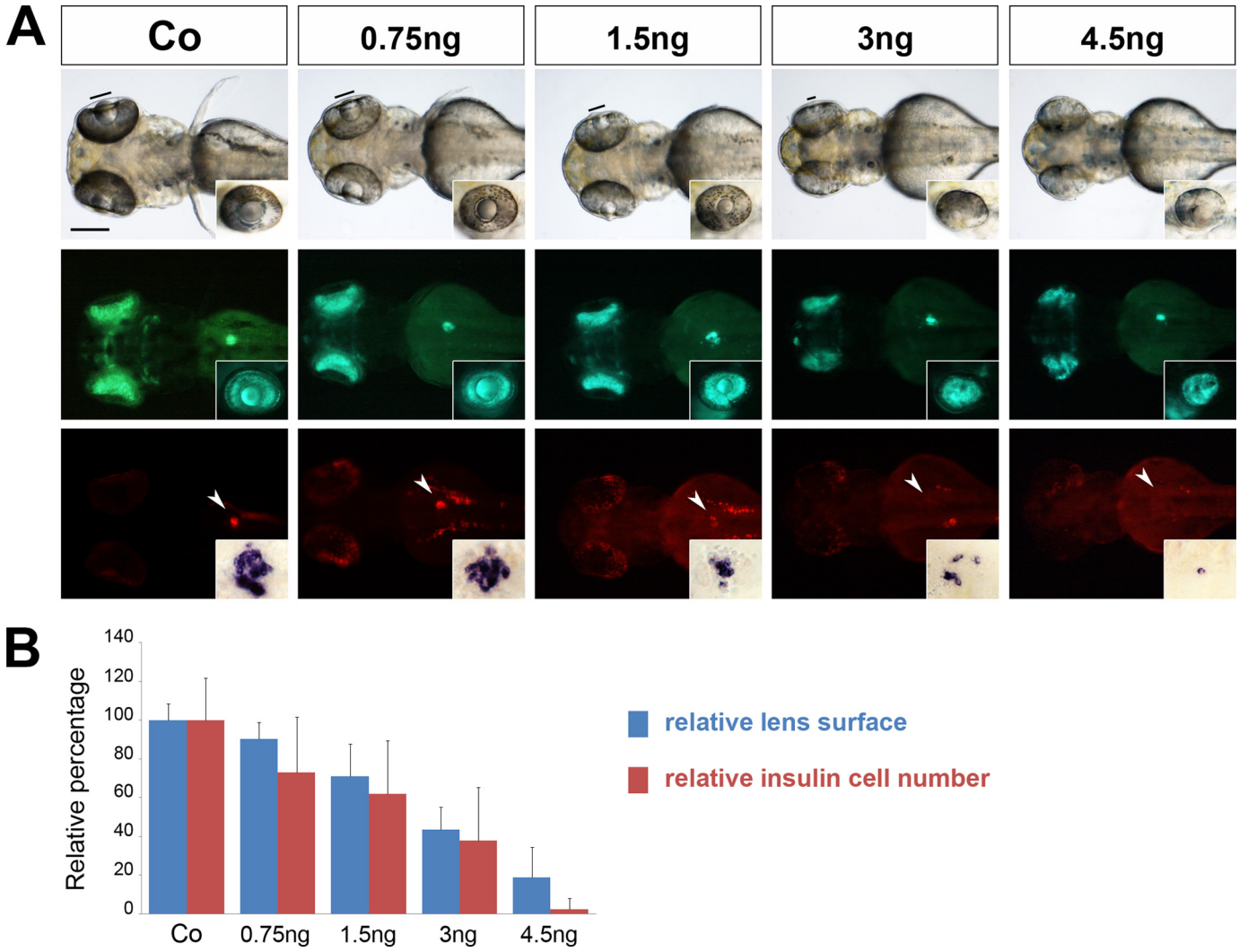

FIGURE 3. **Lens size and β cell number are controlled by similar Pax6b activity levels.** *A*, injection of increasing doses of *pax6b* Mo2 (from 0.75 to 4.5 ng/embryo) leads to progressive reduction of the lens size (*black lines*, *top panels*) and of β cell number (*bottom panels*), whereas the total number of endocrine pancreatic cells expressing the *pax6b*:*GFP* transgene is not significantly altered (*middle panels*). Insulin expression was determined both by expression of the insulin:*dsRed* transgene and by *in situ* hybridization (inlets in the *bottom panels*). The anterior part of 3-dpf embryos is shown, with the anterior side to the *left*. *Scale bars*, 200 μm. *B*, lens surface was measured in the lateral view, and insulin-expressing cells were counted in injected embryos for each condition. Means for control embryos were taken as 100%, and relative percentages were calculated for the injected embryos. *Error bars*, S.D. *Co*, control embryos.

transcripts should lead to removal of the N-terminal part of the homeodomain without causing a frameshift in the coding region. To determine the splicing defects generated by morpholino injection, RNA extracted from morphants and from uninjected control embryos was subjected to RT-PCR designed to amplify a *pax6b* cDNA region corresponding to the HD. To that end, one pair of primers was used (see the *blue arrows* in the *top panel* of Fig. 4), and the amplicons were analyzed directly by sequencing and gel electrophoresis (see the *bottom panels* in Fig. 4). The injection of Mo3 alone, encompassing the exon 8-intron 8 junction, efficiently disrupted splicing at this site, as revealed by the slightly larger amplified cDNA fragment. Direct sequencing of this amplicon revealed the insertion of the first 22 bp of intron 8 in the majority of *pax6b* transcripts. This insertion leads to a frameshift in the coding sequence, generating nine added codons followed by a stop codon 4 bp downstream from the insertion. Thus, we can infer that Mo3 morphants express a Pax6b protein containing the paired domain and the linker region but lacking the C-terminal transactivation domain and a functional homeodomain (see schematic representations of Pax6b protein in Fig. 4). In zebrafish embryos injected with a mixture of the Mo3 and Mo4 morpholinos, *pax6b* transcripts displayed only a deletion of exon 8, as shown by gel electrophoresis and direct sequencing. Because this deletion does not cause a frameshift, translation of these transcripts results in synthesis of a Pax6b protein containing the paired domain and the C-terminal transactivation domain but lacking the C-terminal part of the linker region and the N-terminal part of the homeodomain. Western blotting using a Pax6 antibody raised against the C-terminal domain confirmed the expression of this truncated Pax6b protein in Mo3+Mo4 morphants (supplemental Fig. S3). When eye morphology and the number of pancreatic β cells were examined in these morphants (Fig. 5), the lens appeared significantly reduced in size in both Mo3 and Mo3 + Mo4

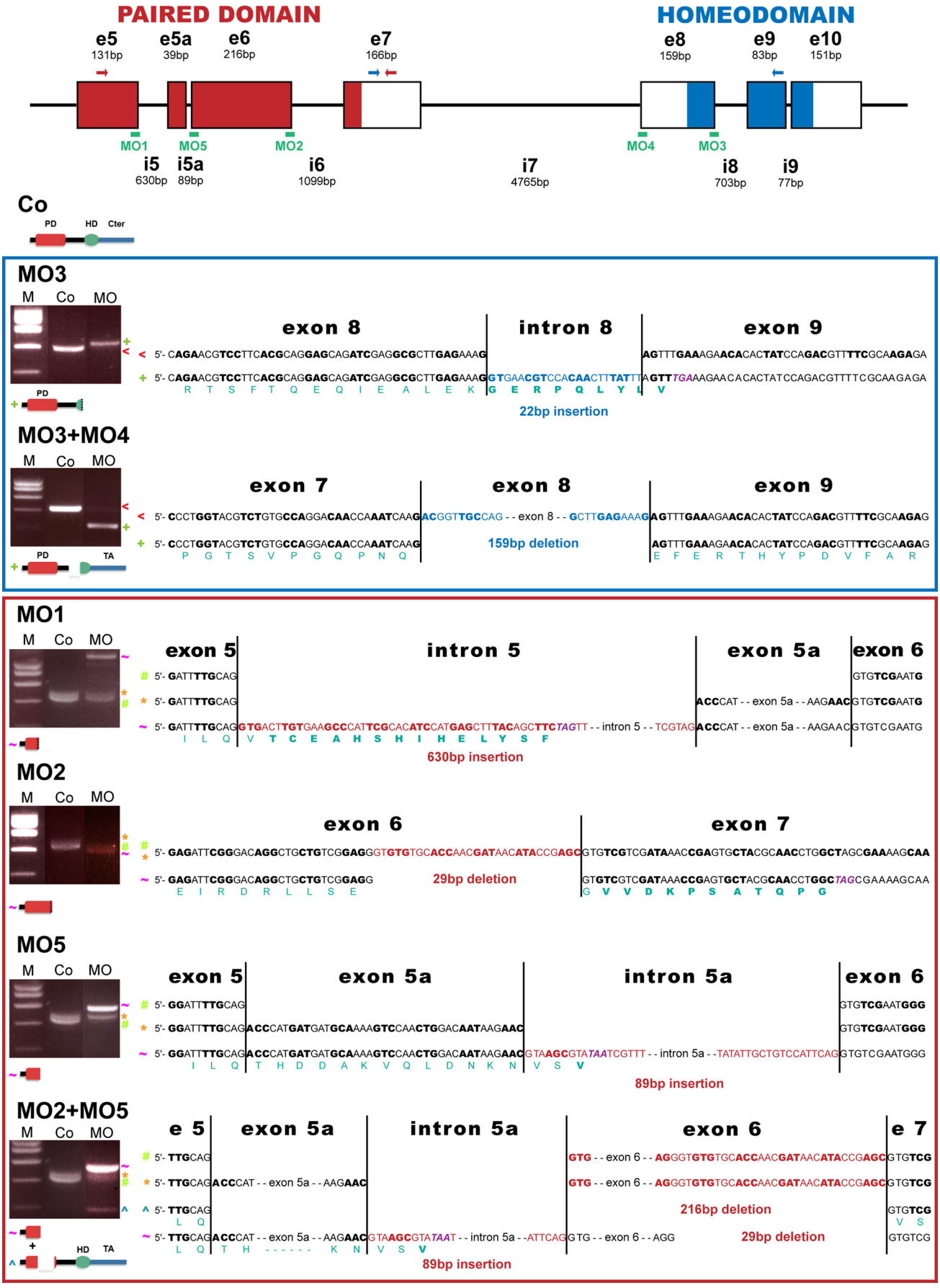

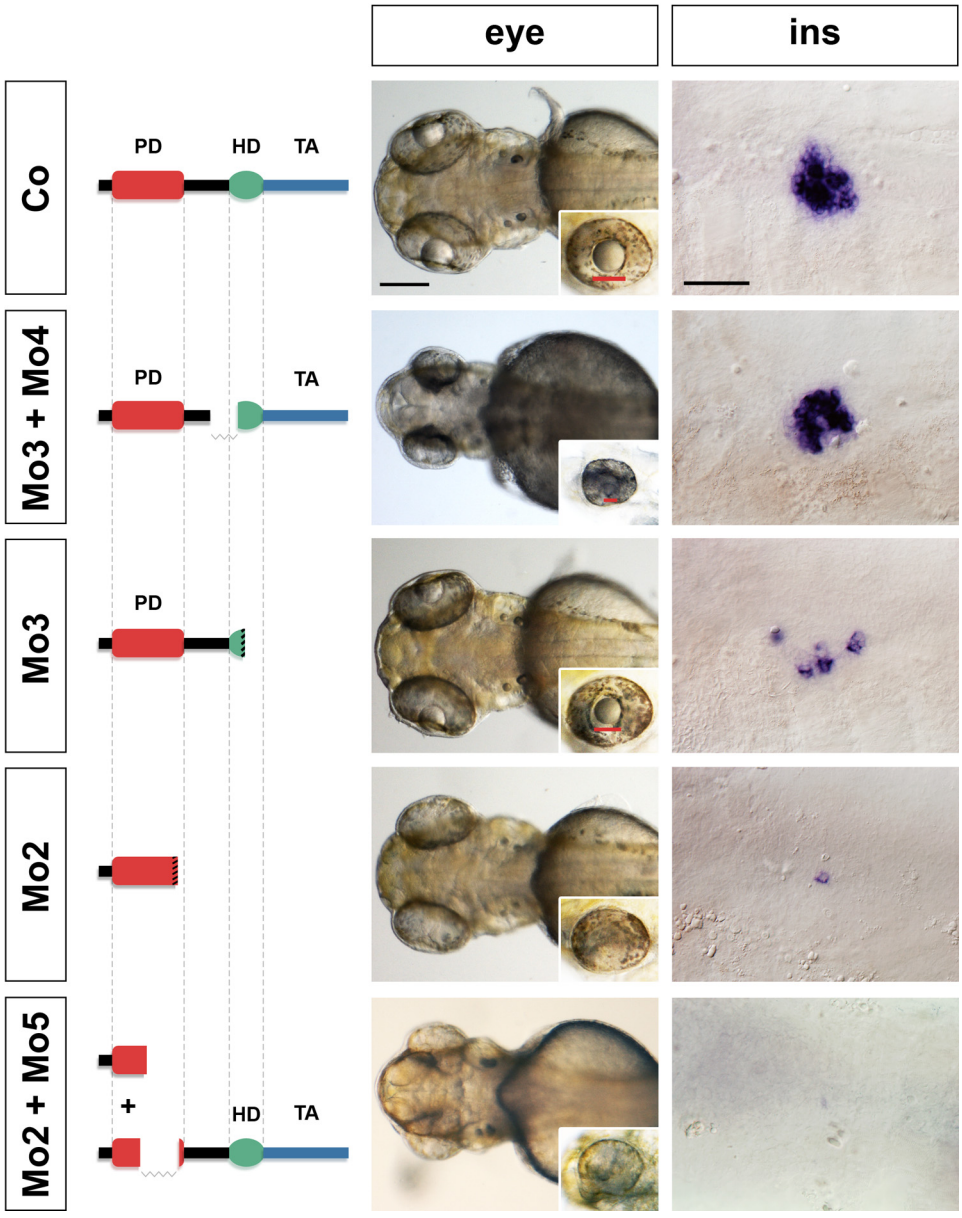

FIGURE 5. **The Pax6b homeodomain is not required for the differentiation of insulin-expressing cells.** *First column*, Pax6b protein prediction resulting from altered splicing following morpholino injection. *Red*, PD; *green*, HD; *blue*, C-terminal transactivation domain (*TA*). *Second column*, *dorsal views* of the anterior part of injected embryos at 3 dpf and *lateral views* of the eyes in the inlets, with the size of the lens highlighted by a *red line*. *Scale bars*, 200 μm. *Third column*, insulin expression determined by *in situ* hybridization. *Scale bars*, 50 μm. *Co*, control embryos.

morphants, but β cell formation was strongly reduced only in the former. This demonstrates that the Pax6b homeodomain is not essential for β cell differentiation.

We also determined the splicing defects caused by other morpholinos (Mo1, Mo2, and Mo5) designed to affect coding regions within the paired domain. The *pax6b* mRNA was analyzed by RT-PCR, followed by direct sequencing and gel electrophoresis (Fig. 4). Mo1, encompassing the exon 5-intron 5 junction, blocked splicing at this site, causing retention of intron 5. This insertion introduces 14 amino acids and a stop codon just after exon 5. Splicing was not totally blocked at this site, however, because correctly spliced *pax6b* mRNAs were still detected in the Mo1 morphants. Mo2 very efficiently perturbed splicing at the exon 6-intron 6 site for almost all *pax6b* transcripts, causing a 29-bp deletion in exon 6 and leading to a premature stop codon at the level of the paired domain. In the Mo5 morphants, most *pax6b* transcripts were found to contain exon 5a and intron 5a, introducing a stop codon just after it. Co-injection of Mo2 and Mo5 caused specific deletion of exon 6 but only in a minority of *pax6b* transcripts. The bulk of these transcripts possessed the combined modifications caused by Mo2 and Mo5. Thus, we can infer that the Mo2 + Mo5 morphants expressed mainly C-terminal truncated Pax6b proteins with low levels of Pax6b lacking a functional paired domain. RT-PCR analysis also demonstrated that all of the *pax6b* morpholinos affected splicing only at their respective target sites, whereas splicing at the other exon-intron junctions within *pax6b* transcripts or of another mRNA remained unaffected (supplemental Fig. S4). We next analyzed eye morphology and pancreatic cell types in these morphants possessing *pax6b* transcripts disrupted at the

FIGURE 4. ***pax6b* RNA splicing defects generated by injection of morpholinos.** Shown is a schematic representation of *pax6b* gene structure between the fifth exon (*e5*) and the tenth exon (*e10*), with regions coding for the paired domain (*red boxes*) and the homeodomain (*blue boxes*) highlighted. Mo1, Mo5, and Mo2 target splicing junctions within regions coding for the paired domain and Mo3 and Mo4 target junctions within the homeobox (*green lines*). Embryos were injected with Mo1 (6 ng/embryo), Mo2 (4.5 ng/embryo), Mo3 (6 ng/embryo), Mo5 (2 ng/embryo), Mo2 + Mo5 (4.5 + 2 ng/embryo, respectively), and Mo3 + Mo4 (6 + 4 ng/embryo, respectively). The RNA splicing defects caused by the different morpholinos were determined by amplifying the cDNAs corresponding to the paired domain and the homeodomain through RT-PCR with two distinct pairs of primers (*red* and *blue arrows*, respectively) and analyzed by gel electrophoresis and sequencing. The combination of Mo3 and Mo4 leads to deletion of the eighth exon. The predicted Pax6b proteins produced in each morphant are represented at the *bottom* of the corresponding gel pictures. *M*, marker (from *top* to *bottom*, 1 kb, 800 bp, 600 bp, 400 bp, and 200 bp); *Co*, control embryos; *MO*, morpholino-injected embryos. *Purple italic characters*, stop codon. *Green characters*, predicted amino acid sequences with the corresponding non-wild-type amino acids in *boldface type*. *PD*, paired domain; *HD*, homeodomain; *TA*, C-terminal transactivation domain.

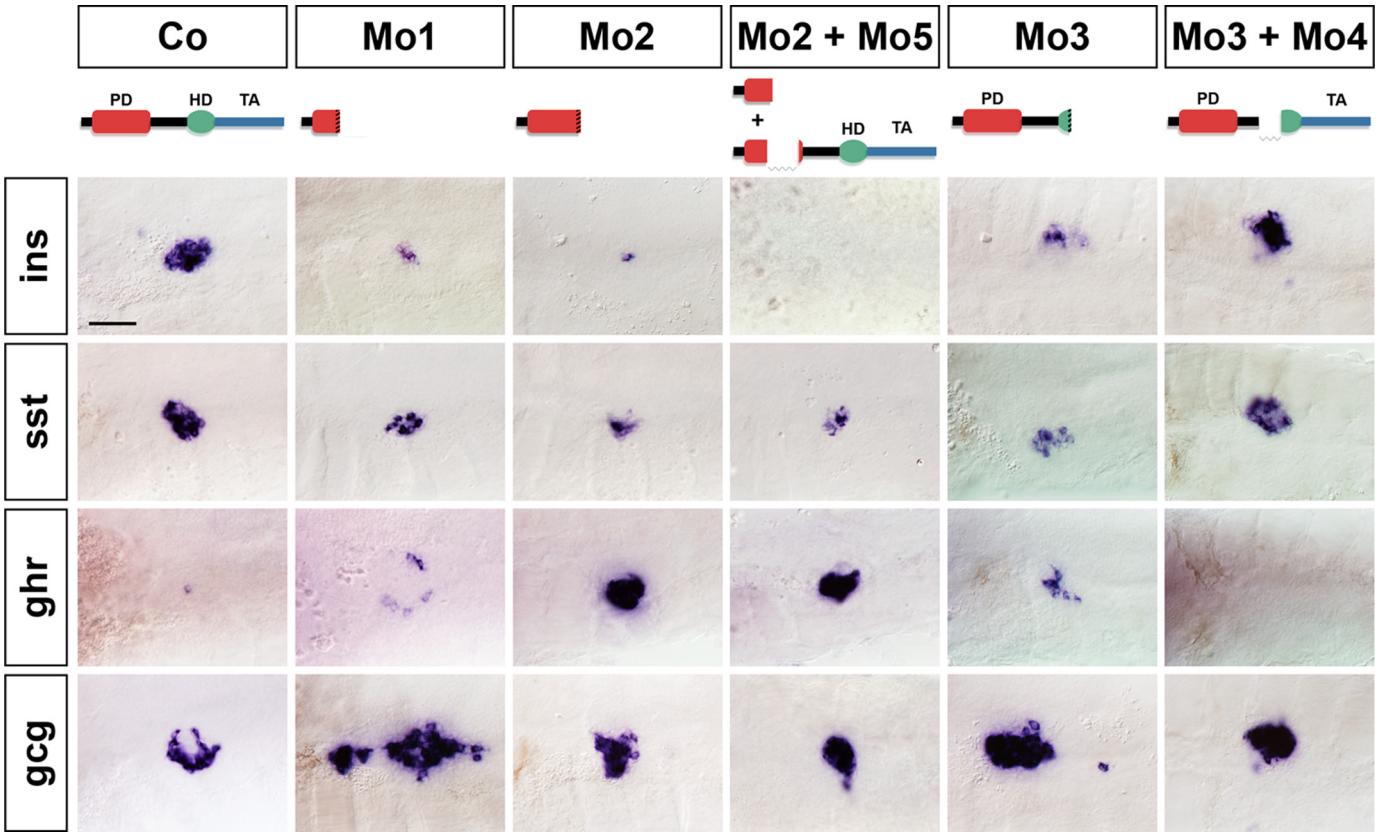

FIGURE 6. **Effects of the different *pax6b* morpholinos on the pancreatic endocrine cell types.** Shown is expression of pancreatic hormone genes as detected by *in situ* hybridization in control (*Co*) and morpholino-injected embryos (*Mo*). Ventral views of the pancreatic area of 3-dpf embryos are shown, with the anterior side to the *left*. *Scale bars*, 50 μm. *ins*, insulin transcripts; *sst*, somatostatin transcripts; *ghr*, ghrelin transcripts; *gcg*, glucagon transcripts.

level of the PD coding sequence. All of them displayed either an absent or a strongly reduced lens (Fig. 5) (data not shown). The Mo2 and Mo2 + Mo5 morphants were found to have no or few β cells (Fig. 5). These data indicate that the whole C-terminal part of the Pax6b protein is crucial for eye and pancreas development.

We also analyzed the other pancreatic endocrine cell types in all of the different *pax6b* morphants (Fig. 6). All of the morphants expected to produce a Pax6b protein deleted in the C-terminal region (Mo1, Mo2, and Mo3) or in the paired domain (Mo2 + Mo5) displayed not only a drastic reduction of β cells but also a significantly decreased number of somatostatin-expressing cells and an increased number of ghrelin-expressing cells. In contrast, the Mo3 + Mo4 morphants expressing a Pax6b protein with a truncated homeodomain did not display any change of β, δ, and ϵ cell numbers compared with the control embryos. Thus, we can conclude that the Pax6b homeodomain is not required for the differentiation of all pancreatic cell types. Thus, these findings explain the phenotypic difference between the *sunrise* mutants and the null *pax6b* mutants/morphants.

Partial Loss of Pax6b Activity Leads to Increased Glucagon Expression—When glucagon expression was analyzed in detail in the *pax6b* morphants, a reproducible increase of α cells was detected especially in the Mo1 morphant; the number of α cells was at least 150% higher on average in the Mo1 morphant compared with control embryos (see Fig. 6). Because the Mo1 morpholino did not disrupt *pax6b* RNA splicing as efficiently as the other morpholinos (see Fig. 4), we wondered if the number of α cells might depend on the levels of endogenous Pax6b protein. This prompted us to analyze the various pancreatic cell types in embryos producing different amounts of functional Pax6b protein. For this, we injected various quantities of the Mo2 morpholino (Fig. 7*A*). As the amount of injected Mo2 increased, the number of insulin$^+$ and somatostatin$^+$ cells gradually decreased. In contrast, the number of glucagon$^+$ cells was found first to increase with a maximum level at 1.5 ng of injected Mo2 morpholino, and then to gradually decrease at higher morpholino doses. The number of ghrelin$^+$ cells was found to rise, appearing maximal at around 3 ng. In order to verify more precisely these effects, quantitative RT-PCRs were performed on RNA extracted from 3-dpf morphants (Fig. 7*B*). The results clearly show that, although the somatostatin and insulin transcripts decreased progressively with the dose of injected Mo2 to reach about 20% (*sst*) and 4% (*ins*), respectively, compared with control embryos, the glucagon transcripts rose to 160% at 1.5 ng of Mo2 and then were down-regulated to about 50% at 4.5 ng of Mo2. In order to quantify more precisely the increase of α cell number, we counted the glucagon-positive cells at 30 hpf because stained cells are more easily discerned at this earlier stage compared with 3 dpf. This analysis showed an increase of about 1.5-fold in the number of α cells after injection of 1.5 ng of Mo2 compared with control embryos (Fig. 7*C*). Thus, these findings reveal the importance of the fine tuning of Pax6 expression level for its biological activity.

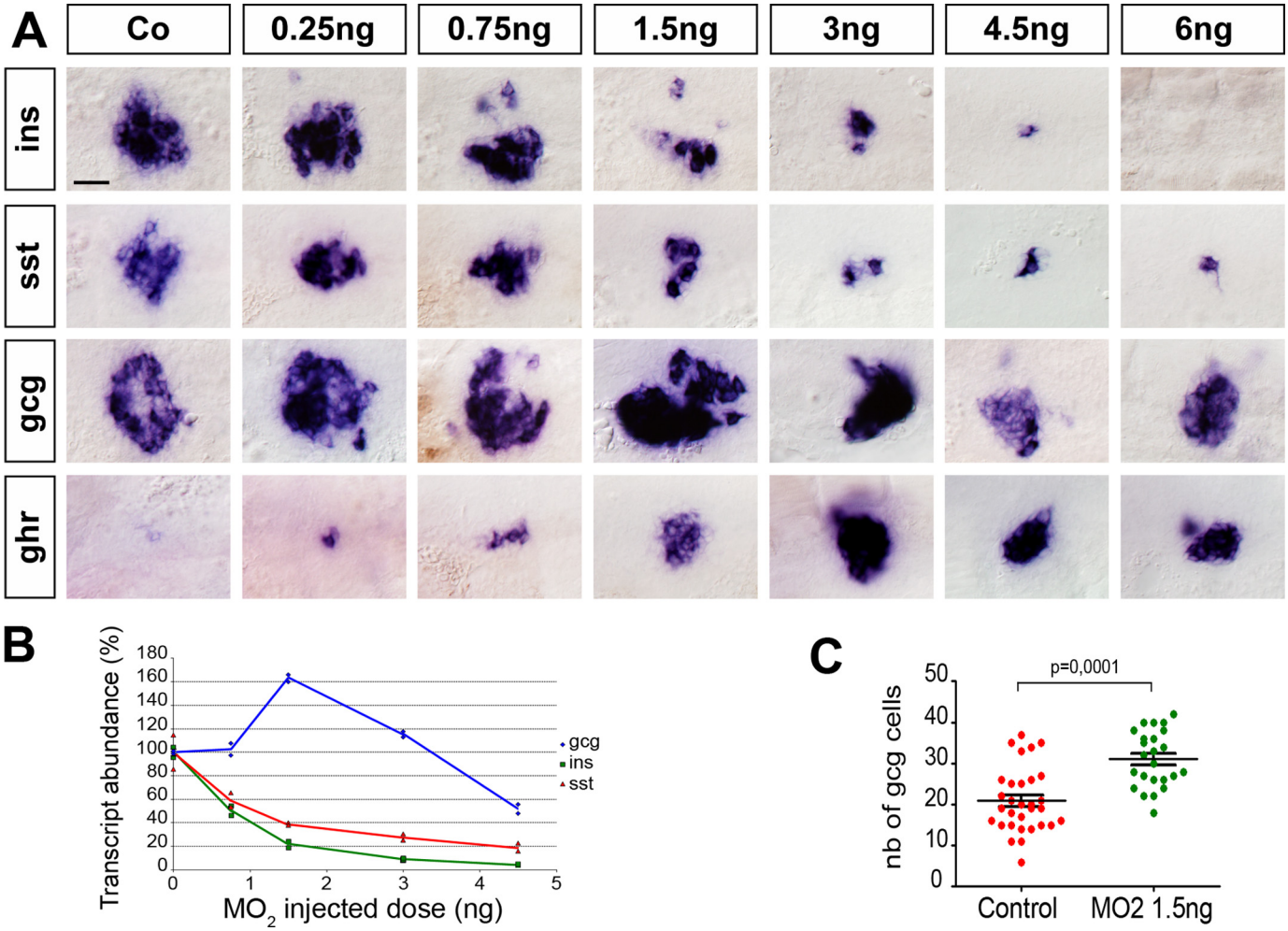

FIGURE 7. **Partial knockdown of *pax6b* leads to an increased level of glucagon gene expression.** *A*, hormone gene expression pattern determined by *in situ* hybridization following injection of increasing doses of morpholino Mo2. Ventral views of the pancreatic area of 3-dpf embryos are shown, with the anterior side to the *left*. *Scale bars*, 25 μm. *ins*, insulin transcripts; *sst*, somatostatin transcripts; *ghr*, ghrelin transcripts; *gcg*, glucagon transcripts. *B*, quantitative RT-PCR of glucagon, insulin, and somatostatin transcripts in two independent mRNA preparations from zebrafish embryos injected with various doses of Mo2 morpholinos. *C*, number of glucagon-positive cells in 30-hpf embryos injected with 1.5 ng of control morpholino or of Mo2 morpholino. Each *point* in the graph represents the α cell number of one embryo. Cell counting was performed directly under the microscope at high magnification on whole mount embryos by focusing successively on each layer of stained cells. *Co*, control embryos.

DISCUSSION

We have previously shown that only one of the zebrafish-duplicated *pax6* genes, namely *pax6b*, is expressed in all endocrine cell types of the pancreas (25). We demonstrate here by a morpholino knockdown approach and analysis of the *sunrise* and *pax6b*^{sa0086} zebrafish mutants that *pax6b* is required for proper endocrine cell differentiation, but its homeodomain is not essential for this function. Both the paired domain and the homeodomain are the most conserved parts of Pax6 from invertebrates to vertebrates (5), indicating strong evolutionary pressure to maintain the function of these two DNA-binding domains. However, our data show that a truncation in the Pax6b homeodomain does not disturb pancreas development, whereas this deletion affects the eyes. It is possible that subtle pancreatic defects may not have been detected after deletion of the Pax6b homeodomain, but the fact that *sunrise* homozygous mutants survive to adulthood is a strong argument for a nonessential role of the Pax6b homeodomain in the pancreas. Thus, we can infer that Pax6b regulates expression of target genes in pancreatic cells mostly, if not exclusively, through DNA binding of its paired domain. By analyzing *Pax6*^{Aey18} and *Pax6*^{Neu4} mutant mice, possessing a mutated paired domain and a mutated homeodomain, respectively, Haubst *et al.* (18) have previously drawn similar conclusions for the action of PAX6 in the murine brain cortex. Altogether, these data indicate that the Pax6 homeodomain is important for eye development in mammals and fish. In contrast, in *Drosophila*, eye development can be triggered by a Pax6 protein devoid of the entire homeodomain (33), suggesting that the role of the homeodomain in the eye has been acquired during vertebrate evolution.

Our study also highlights the usefulness of morpholinos targeting exon-intron junctions, allowing the generation of various truncations in a studied protein within zebrafish embryos, thereby revealing the role of specific parts of a protein *in vivo*. When a single morpholino was injected in zebrafish eggs, the splicing process was disturbed specifically at the targeted junction site, either leading to the presence of the intronic sequence within the final transcript or leading to the use of nearby cryptic

donor/acceptor splicing sites. Importantly, this work reveals for the first time that the combined injection of two morpholinos targeting the two splicing sites flanking the same exon can induce the specific removal of this exon from the spliced transcript. The efficiency of such a deletion seems to vary among the splicing sites because, on the two tested *pax6b* exons, one (exon 8) was deleted with a high efficiency, whereas the other (exon 6) was removed only in a minority of *pax6b* transcripts. The fact that the pancreatic endocrine defects caused by the injection of morpholino Mo3 were rescued by the combined injection of morpholino Mo4 clearly demonstrates that (i) the homeodomain is not essential in pancreas and (ii) the endocrine defects obtained by the Mo3 injection are due to *pax6b* knockdown and not to other nonspecific Mo3 off targets. In addition, the fact that the same pancreatic perturbations were observed with three different *pax6b* morpholinos and were also detected in the *pax6b*^{sa0086} mutant further consolidates the validity of our morpholino knockdown data. The only difference noted between the *pax6b*^{sa0086} mutants and the *pax6b* morphants is a reduction of glucagon-expressing α cells, which was observed in 40% of mutants, whereas α cells were not significantly affected after injection of 4.5 ng of Mo2 morpholino. This slight divergence may be due to a small residual expression of Pax6b in morphants that would be sufficient to drive α cell differentiation. On the other hand, the fact that α cell differentiation is not strongly affected in about 60% of *pax6b*^{sa0086} mutants indicates that a Pax6b-independent pathway may also be used to generate glucagon cells. The variation in α cell number, as well as in δ cells and in lens size, observed among *pax6b*^{sa0086} mutants could be due to a different genetic background in each mutant embryo. Indeed, the *pax6b*^{sa0086} fish have been recently identified following ethylnitrosurea large scale mutagenesis, and it is possible that other loci influence the phenotype severity of *pax6b*^{sa0086} homozygotes. Several outcrosses of the *pax6b*^{sa0086} mutant will be necessary to verify this hypothesis.

Another unexpected and important finding of this study is the increase in glucagon expression after partial *pax6b* knockdown. This increase of α cells was initially noticed after injection of the Mo1 *pax6b* morpholino. Because this morpholino was much less efficient for disrupting *pax6b* splicing compared with the other *pax6b* morpholinos (see Figs. 4 and 6), this prompted us to inject various amounts of the more efficient Mo2 morpholino. This dose-response analysis revealed that the increase of α cells and of glucagon transcripts was maximal with 1.5 ng of injected Mo2 corresponding to a mild reduction of *pax6b* activity. Previous studies have shown that a precise range of the Pax6 protein level is important for the proper development of the eyes, brain, and pancreas because an increase of *Pax6* expression in transgenic mice leads to abnormalities in these organs (19, 20, 34). Moreover, heterozygous Pax6 individuals display anomalies in eye morphology and brain patterning (10). However, no obvious morphological abnormality has been reported yet at the level of the pancreas in Pax6 heterozygous mice, and we did not detect any obvious anomalies in *pax6b*^{sa0086} heterozygous larvae (data not shown). Recently, pancreatic expression of the prohormone convertases *PC1/3* has been reported to be down-regulated in *Pax6* heterozygous mice, thereby contributing to the abnormal glucose metabolism (12). This example indicates that a 50% reduction of Pax6 levels is sufficient to perturb expression of some pancreatic target genes. However, our observation of the increase of α cells after partial knockdown of *pax6b* is quite peculiar because this effect is not occurring after full knockdown of *pax6b*. A similar phenomenon has recently been shown for the pancreatic transcription factor Ptf1a. Indeed, a partial reduction of Ptf1a levels in zebrafish embryos strongly promotes endocrine cell fate, whereas such an effect is not observed when Ptf1a is completely repressed (27). The precise molecular mechanisms determining the formation of distinct endocrine cell types from pancreatic progenitor cells are still largely unknown. Our data indicate that the precise levels of Pax6 protein may be one of the clues for pancreatic cell fate choice. This also highlights the importance of carefully monitoring transcription factor levels when rescue or gain-of-function experiments are performed.

Acknowledgments—We thank W. Driever, S. Leach, and M. Parsons for providing the insulin:dsRed and ptf1a:GFP zebrafish transgenic lines. For providing the zebrafish pax6b knock-out allele sa0086, we thank the Hubrecht laboratory and the Sanger Institute Zebrafish Mutation Resource (ZF_MODELS Integrated project; Contract LSHG-CT-2003-503496; funded by the European Commission) also sponsored by the Wellcome Trust (Grant WT 077047/Z/05/Z). We especially thank Elisabeth Bush for collecting, fixing, and sending all pax6b mutant clutches. The results of sequencing and confocal imaging were obtained thanks to V. Dhennin and S. Ormenèse, respectively (Genotranscriptomics and Imaging Platforms, respectively, GIGA, University of Liège). The zebrafish lines were raised with the help of M. Winandy (Zebrafish Facility and Transgenics Platform, GIGA, University of Liège).

REFERENCES

1. Quiring, R., Walldorf, U., Kloter, U., and Gehring, W. J. (1994) *Science* **265,** 785–789
2. Kioussi, C., O'Connell, S., St-Onge, L., Treier, M., Gleiberman, A. S., Gruss, P., and Rosenfeld, M. G. (1999) *Proc. Natl. Acad. Sci. U.S.A.* **96,** 14378–14382
3. Dohrmann, C., Gruss, P., and Lemaire, L. (2000) *Mech. Dev.* **92,** 47–54
4. Chi, N., and Epstein, J. A. (2002) *Trends Genet.* **18,** 41–47
5. Callaerts, P., Halder, G., and Gehring, W. J. (1997) *Annu. Rev. Neurosci.* **20,** 483–532
6. Matsuo, T., Osumi-Yamashita, N., Noji, S., Ohuchi, H., Koyama, E., Myokai, F., Matsuo, N., Taniguchi, S., Doi, H., and Iseki, S. (1993) *Nat. Genet.* **3,** 299–304
7. Hill, R. E., Favor, J., Hogan, B. L., Ton, C. C., Saunders, G. F., Hanson, I. M., Prosser, J., Jordan, T., Hastie, N. D., and van Heyningen, V. (1991) *Nature* **354,** 522–525
8. Favor, J., Peters, H., Hermann, T., Schmahl, W., Chatterjee, B., Neuhäuser-Klaus, A., and Sandulache, R. (2001) *Genetics* **159,** 1689–1700
9. St-Onge, L., Sosa-Pineda, B., Chowdhury, K., Mansouri, A., and Gruss, P. (1997) *Nature* **387,** 406–409
10. Sisodiya, S. M., Free, S. L., Williamson, K. A., Mitchell, T. N., Willis, C., Stevens, J. M., Kendall, B. E., Shorvon, S. D., Hanson, I. M., Moore, A. T., and van Heyningen, V. (2001) *Nat. Genet.* **28,** 214–216
11. Manuel, M., and Price, D. J. (2005) *Brain Res. Bull.* **66,** 387–393
12. Wen, J. H., Chen, Y. Y., Song, S. J., Ding, J., Gao, Y., Hu, Q. K., Feng, R. P., Liu, Y. Z., Ren, G. C., Zhang, C. Y., Hong, T. P., Gao, X., and Li, L. S. (2009) *Diabetologia* **52,** 504–513
13. Ding, J., Gao, Y., Zhao, J., Yan, H., Guo, S. Y., Zhang, Q. X., Li, L. S., and Gao, X. (2009) *Endocrinology* **150,** 2136–2144

14. Simpson, T. I., and Price, D. J. (2002) *BioEssays* **24,** 1041–1051
15. Sander, M., Neubüser, A., Kalamaras, J., Ee, H. C., Martin, G. R., and German, M. S. (1997) *Genes Dev.* **11,** 1662–1673
16. Nomura, T., and Osumi, N. (2004) *Development* **131,** 787–796
17. Nomura, T., Haba, H., and Osumi, N. (2007) *Dev. Growth Differ.* **49,** 683–690
18. Haubst, N., Berger, J., Radjendirane, V., Graw, J., Favor, J., Saunders, G. F., Stoykova, A., and Götz, M. (2004) *Development* **131,** 6131–6140
19. Yamaoka, T., Yano, M., Yamada, T., Matsushita, T., Moritani, M., Ii, S., Yoshimoto, K., Hata, J., and Itakura, M. (2000) *Diabetologia* **43,** 332–339
20. Schedl, A., Ross, A., Lee, M., Engelkamp, D., Rashbass, P., van Heyningen, V., and Hastie, N. D. (1996) *Cell* **86,** 71–82
21. Sansom, S. N., Griffiths, D. S., Faedo, A., Kleinjan, D. J., Ruan, Y., Smith, J., van Heyningen, V., Rubenstein, J. L., and Livesey, F. J. (2009) *PLoS Genet.* **5,** e1000511
22. Heller, R. S., Stoffers, D. A., Liu, A., Schedl, A., Crenshaw, E. B., 3rd, Madsen, O. D., and Serup, P. (2004) *Dev. Biol.* **268,** 123–134
23. Heller, R. S., Jenny, M., Collombat, P., Mansouri, A., Tomasetto, C., Madsen, O. D., Mellitzer, G., Gradwohl, G., and Serup, P. (2005) *Dev. Biol.* **286,** 217–224
24. Kleinjan, D. A., Bancewicz, R. M., Gautier, P., Dahm, R., Schonthaler, H. B., Damante, G., Seawright, A., Hever, A. M., Yeyati, P. L., van Heyningen, V., and Coutinho, P. (2008) *PLoS Genet.* **4,** e29
25. Delporte, F. M., Pasque, V., Devos, N., Manfroid, I., Voz, M. L., Motte, P., Biemar, F., Martial, J. A., and Peers, B. (2008) *BMC Dev. Biol.* **8,** 53
26. Godinho, L., Williams, P. R., Claassen, Y., Provost, E., Leach, S. D., Kamermans, M., and Wong, R. O. (2007) *Neuron* **56,** 597–603
27. Dong, P. D., Provost, E., Leach, S. D., and Stainier, D. Y. (2008) *Genes Dev.* **22,** 1445–1450
28. Kimmel, C. B., Ballard, W. W., Kimmel, S. R., Ullmann, B., and Schilling, T. F. (1995) *Dev. Dyn.* **203,** 253–310
29. Hauptmann, G., and Gerster, T. (1994) *Trends Genet.* **10,** 266
30. Argenton, F., Zecchin, E., and Bortolussi, M. (1999) *Mech. Dev.* **87,** 217–221
31. Milewski, W. M., Duguay, S. J., Chan, S. J., and Steiner, D. F. (1998) *Endocrinology* **139,** 1440–1449
32. Devos, N., Deflorian, G., Biemar, F., Bortolussi, M., Martial, J. A., Peers, B., and Argenton, F. (2002) *Mech. Dev.* **115,** 133–137
33. Punzo, C., Kurata, S., and Gehring, W. J. (2001) *Genes Dev.* **15,** 1716–1723
34. Manuel, M., Georgala, P. A., Carr, C. B., Chanas, S., Kleinjan, D. A., Martynoga, B., Mason, J. O., Molinek, M., Pinson, J., Pratt, T., Quinn, J. C., Simpson, T. I., Tyas, D. A., van Heyningen, V., West, J. D., and Price, D. J. (2007) *Development* **134,** 545–555
35. Westerfield, M. (2000) *The Zebrafish Book*: *A Guide for the Laboratory Use of Zebrafish* (*Danio rerio*), 4th Ed., University of Oregon Press, Eugene, OR